25 Conducting solids

R. K. B. Gover[a] **and P. R. Slater**[b]

[a] *School of Chemistry, University of Durham, Durham, UK DH1 3LE*
[b] *Department of Chemistry, University of Surrey, Guildford, Surrey, UK GU2 7XH*

Fujiwara *et al*. have developed a novel method for preparing crystalline $LiCoO_2$ cathode films on paper using an electrodeposition method from solutions of LiOH and $CoSO_4$ at 120 °C. This year has also seen a move toward hybrid lithium anode materials by a number of different research groups, with interesting electrochemical properties being reported for a wide range of materials.

In terms of solid oxide fuel cell (SOFC) research, fluorite-type electrolytes (such as yttria stabilised zirconia) have long dominated the area. Alternative electrolyte materials are however rapidly growing in stature, and represent key highlights of the research in 2002. In particular, promising results from single cell SOFCs based on doped $LaGaO_3$ have been reported by Ishihara *et al*. Promising oxide ion conductivity has also been reported in apatite-type oxides by a number of groups.

In terms of superconductivity research, lithium has been shown to be superconducting under high pressure, with T_c's as high as 20 K, which represents the highest T_c for any element.

1 Introduction

This year's report will follow the same basic format as last year: the first section examines the recent advances made in the field of Li ion battery chemistry. This is followed by materials that have applications in solid oxide fuel cells, with the final sections of the report focusing on other ionic conductors and superconducting materials.

2 Lithium ion cells

A literature search using the search term "Li ion batteries" was used to produce Fig. 1 presented below. This figure shows that since 1994 there has been a drastic increase in the number of papers published on aspects of Li ion batteries. This year is no exception, with an examination of the year's literature showing that Li ion battery research is still a thriving area of research, with many new materials being reported and improvements being made to established materials

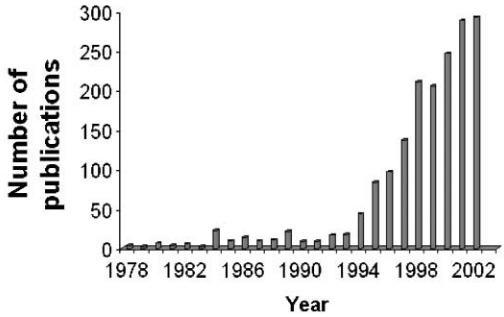

Fig. 1 Number of publications published as a function of year using the search term "Li ion batteries."

Research this year has shown a move towards hybrid materials, and this is especially noticeable for anodes. This is most likely due to the higher theoretical capacities that can be obtained with metal alloys compared to the established carbon materials. Preparation of hybrid materials will perhaps allow commercialisation of materials that have the favourable aspects of these types of materials.

Morcrette and co-workers have published a paper that may be of general interest to groups that perform *in-situ* X-ray powder diffraction measurements on a variety of battery materials.[1] The paper outlines the variety of different methods employed in the past, problems encountered and also describes the recent advances made in instrumentation and *in-situ* cell design. These recent advances have been used to examine PNb_9O_{25} and $LiCoO_2$. The paper also briefly discusses the growing importance of other techniques such as XANES, Mossbauer and Raman spectroscopy for *in-situ* studies on Li ion cells.

3 Anodes

This year has seen a number of review articles on a variety of different aspects of anode chemistry. A review of carbon anodes and the criteria required when selecting suitable carbon for Li ion battery applications was published by Kinoshita and Zaghib.[2] Aurbach and co-workers have reviewed the failure mechanisms of lithium metal and lithiated graphite anodes in liquid electrolyte solutions.[3] A review of nano-alloy anodes was presented by Li *et al*.[4] This review summarizes the recent studies on nano SnSb alloys and also describes a method of preparing carbon/nano-alloys.

4 Carbon anodes

Yang *et al*. have examined Li intercalation into raw acid oxidised carbon nanotubes.[5] This paper reports the preparation of the carbon nanotubes and subsequent treatment of these materials using mixed solutions of HNO_3 and H_2SO_4. The authors reported initial capacities of about 600 mAh g^{-1} with reversible capacities of 200 mAh g^{-1}. It was found that the acid oxidation determined the nature of the electrode

interface formed between the carbon and the electrolyte, and highlighted the effects of the acid oxidation on the nature of the interface and its effect on the observed capacities.

Abe and co-workers have reported graphitised carbon thin films prepared using plasma-assisted chemical vapour deposition methods.[6] The films were found to be flat, free from pin hole defects, with the films orientated along the *c* axis. Electrochemically the properties were found to be similar to those found in commercial graphite electrodes.

Azais *et al*. have examined the effects of reactive milling of lithium with graphites and their application in lithium ion cells.[7] These materials were tested as anodes and showed higher reversible capacities than milled graphites prepared under identical conditions. The authors explained the improvement in properties of the milled lithium/graphites as being due to the formation of lithiated surface films.

The effects of copolymer encapsulation of graphite have been explored by Pan and co-workers with the aim of reducing the irreversible capacity and improving the cycling performance.[8] The graphite was encapsulated with an ionically conducting copolymer using radiation initiated polymerisation. It was noted that materials prepared in this fashion improved the initial efficiency and cycling performance compared to natural graphite. The authors used Raman spectroscopy to probe the differences between the hybrid material and natural graphites and found that encapsulation depressed some of the structural changes induced by the co-intercalation of solvent molecules. It was also noted that the resistance of these materials was stable during repeated cycling, which supports the results obtained from Raman spectroscopy. Discharge capacities of ~320 mAh g^{-1} were observed for the copolymer encapsulated sample compared to ~280 mAh g^{-1} for untreated samples.

2-Vinylpyridine has been examined as an additive in graphite/$LiMn_2O_4$ cells stored at temperatures greater than 50 °C.[9] The degradation mechanism in these cells is mainly due to the reduction of Mn^{2+} dissolved from the spinel material. On dissolution of Mn^{2+} into the electrolyte, the graphite anode undergoes an irreversible electrochemical reaction at the interface between the graphite and the electrolyte leading to a gradual degradation in the cell's properties. Addition of 2-vinylpyridine was seen to suppress the degradation of the graphite and hence an improvement is seen in the properties.

Zhang and Jow have evaluated the stability of acrylonitrile-methyl methacrylate (AMMA) as a binder for use in graphite electrodes and compared its properties to polyvinylidene difluoride (PVDF).[10] Due to the higher chemical stability of AMMA with respect to lithiated graphite, it was observed that the electrolyte surface interface film formed was more stable, and this improves the storage performance of the cells.

5 Non-carbon anodes

Alloys

Tostmann and co-workers have investigated the electrochemically induced phase changes in lithium doped InSb alloys using *in-situ* X-ray absorption studies.[11] In this work the authors reported the results of a comprehensive analysis of X-ray

absorption data collected during cycling of a sample of InSb. It was reported that on discharge indium is replaced by lithium, with about 90% of the indium removed from the zinc blende type structure. In the fully charged state about 40% of the indium remains as metal with a corresponding number of defects present in the $In_{1-y}Sb$ alloy. The stability of the electrochemically prepared material is attributed to the Sb fcc sublattice. Wachtler *et al*. have prepared Sn–Sb, Sn–Ag, Sb–Ag and Sn–Sb alloys using chemical precipitation methods with $NaBH_4$, with the electrochemical properties of these alloys examined extensively.[12] SnSb and Sn/SnSb alloys were found to give capacities of 500 and 600 mAh g^{-1} for more than 30 cycles. However all of the materials examined exhibited large irreversible capacities in the first cycle.

Tamura and co-workers have also examined powdered Sn and thin film Sn/Cu materials for applications in lithium ion cells.[13] This group focused on fabricating anodes by annealing the deposited anodes on copper foils, and then compared the resultant materials to normal tin powders. Although the capacities of the films and powders were found to be similar (~930m Ah g^{-1}), the capacity retention of these films was found to be of the order of 94%, which is a significant improvement over the 20% seen for powdered materials. This improvement has been attributed to the formation of different intermetallic layers between the tin and the copper current collector, which gives superior stability on repeated charge/discharge cycles.

Mg_2Si has been prepared by mechanically activated annealing and its electrochemical properties evaluated by Roberts.[14] When the discharge limits were between 5–650 mV, capacity in the region of 800 mAh g^{-1} was observed although rapid capacity fading was noted. When the voltage limits were set at 50–225 mV a stable discharge capacity of 100 mAh g^{-1} was observed. X-Ray diffraction indicated the formation of Li_2MgSi after lithium insertion.

Monconduit and co-workers have examined the cycling properties of $Co_{1-2y}Fe_yNi_ySb_3$ ($0.125 < y < 0.5$) compounds in lithium cells.[15] Structure analysis by the Rietveld method using X-ray powder diffraction data confirmed that all materials prepared have the skutterudite structure. The first discharge cycle shows two plateaus; the higher potential, which occurs at approximately 0.8 V, has a capacity of approximately 150–250 mAh g^{-1} and is dependent on the value of y. The second plateau occurs from 0.5 to 0.6 V and is due to Li–Sb alloy formation. However, on charging of the cell only the second plateau can be utilized and this agrees well with other studies on the alloying of Li and Sb. After 20 cycles a stable capacity of 100 mAh g^{-1} was observed.

Li_xVM_4 (M = P and As) has been examined as a potential anode by Doublet.[16] The results presented showed that the capacities of these materials was dependent on M with a value of 550 mAh g^{-1} observed for Li_xVP_4 materials and 530 mAh g^{-1} for Li_xVAs_4 materials. It was also noted that this materials has very low volume changes (<1%) on cycling, making it an attractive alternative to metal alloys.

Pralong *et al*. have examined Li uptake into CoP_3 and found a reversible capacity of the order of 400 mAh g^{-1}.[17] X-Ray diffraction, electron microscopy and electrochemical measurements coupled with XPS measurements showed that, as lithium was inserted into the material, a mixture of Li_3P and Co clusters formed. Extraction of Li from this ionic conducting Co matrix gave particles of LiP.

Oxides

Yang *et al*. have examined the properties of SiO_{2-x} anodes with work investigating the effects of particle size and oxygen contents.[18] Exceptionally high capacities of the order of 1600 mAh g^{-1} were found for the composition $SiO_{0.8}$ in the voltage range 0.02 to 1.4 V. The capacity was seen to drop as the oxygen content increased.

Aurbach *et al.* have reported the preparation of SnO nanoparticles using sonochemical methods.[19] Samples were prepared using mildly basic solutions of $SnCl_2$ and were found to produce an amorphous material. This amorphous material can then be transformed to nanoparticles of SnO by heating at temperatures in the region of 200 °C. Electrochemical analysis of the amorphous materials and nanoparticles was performed, with the nanoparticles found to give superior initial capacities (~790 mAh g^{-1}). Surface effects were thought to be the cause of the large irreversible capacities observed.

Martos *et al*. have reported the preparation of $Sn_{1-x}Mo_xO_2$ materials synthesised by mechanochemical mixing with agate ball and jars.[20] The results suggest that Mo doped samples formed with Mo^{4+}. The addition of Mo is found to improve discharge capacity retention, with a capacity of ~250 mAh g^{-1} after 25 cycles observed (efficiency ~64%) compared with ~200 mAh g^{-1} for the undoped materials (efficiency ~42%). The improvement is thought to be due to the formation of a Li–Mo–O conducting matrix during lithium insertion. Si was found to be present in the samples, which is thought to have come from the experimental apparatus. It was suggested that the presence of Si improved the observed electrochemical properties.

$Mn_{1-x}Mo_{2x}V_{2(1-x)}O_6$ has been examined by Hara *et al.*[21] for potential use in Li ion anodes. Samples were prepared from Mn_2O_3, V_2O_5, and MoO_3 using classical solid state methods. The electrochemical properties of these materials are affected by the Mo doping with the $Mn_{0.6}Mo_{0.8}V_{1.2}O_6$ exhibiting charge-discharge capacities of 1400 mAh g^{-1} compared to that of the parent MnV_2O_6 material (1000 mAh g^{-1}). Kim *et al*. have examined $MnMoO_4$, prepared using conventional solid state reaction methods.[22] Discharge capacities of 800 mAh g^{-1} were recorded before irreversible conversion to an amorphous material occurred. Capacity retention was quoted as being good.

Behm and Irvine have presented the result of comprehensive studies on a number of tin based compounds that may be suitable as anodes in Li ion cells.[23] In this paper the properties of cubic and layered SnP_2O_7, $LiSn_2(PO_4)_3$, $Sn_2P_2O_7$, $Sn_3(PO_4)_2$ and amorphous Sn_2BPO_6 were examined. The best material was cubic SnP_2O_7, which showed capacities of 360 mAh g^{-1} with a capacity retention of 96% (when charged between 0.02 and 1.2 V). Conversion to amorphous materials was observed during cycling.

Palos *et al*. have examined amorphous $FeBO_3$ and found that it can intercalate 3 Li ions per formula unit at 1.1 V.[24] A capacity of 300 mAh g^{-1} was obtained when the material was cycled between 1.5 and 3 V. Wang and coworkers have examined the cobalt oxides CoO and Co_3O_4 as potential anodes.[25,26]. They found that CoO had a usable capacity of about 300 mAh g^{-1} whereas Co_3O_4 had capacities of about 360 mAh g^{-1}.

Hybrid materials

Li *et al*. have prepared nanosized SnSb particles pinned to the surface of micrometer sized carbon spheres using co-precipitation methods.[27] It was found that this material was better than either carbon or alloys alone, with the improvement attributed to the alloy particle size, good dispersion and tight pinning of the alloy particles to the surface of the carbon spheres. Capacities of the order of 500 mAh g^{-1} were achieved with 99% efficiency over 35 cycles.

Chen *et al*. have examined carbon nanotube Sn_2Sb nanocomposites.[28] The nanocomposites of carbon nanotubes (CNT)/Sn_2Sb were prepared by reduction of $SnCl_2$ and $SbCl_3$ in the presence of the carbon nanotubes. The samples were examined using both scanning and transmission electron microscopy, and showed that the majority of the metal particles were to be found in the CNT web, with a small amount found on the outside surfaces of the CNT's. Electrochemical testing showed that higher specific capacities could be achieved than with pristine CNT's with better cyclability than normally seen for unsupported Sn_2Sb materials. A capacity of ~580 mAh g^{-1} was achieved from CNT-56 weight % Sn_2Sb material, decreasing to 370 mAh g^{-1} after 80 deep charge/discharge cycles.

Egashira and co-workers have examined activated carbon fibres, which contain Sn nanoparticles.[29] Activated carbon fibres were impregnated with tin nanoparticles, with the particle size of the tin controlled by the surface morphology of the carbon fibres. Capacities of *ca.* 200 mAh g^{-1} were achieved during the first cycle, which is significantly better than achieved from the carbon fibres alone. The authors reported that these materials have excellent cyclability.

Dailly *et al*. have prepared antimony-containing graphite compounds and investigated the electrochemical properties.[30] As would be expected, it was found that lithium intercalated into both the graphite and the alloy giving reversible electrochemical capacities of the order of 700 mAh g^{-1} between 0 and 2 V.

Fujimoto *et al*. have examined the effects of boron addition on the structure and electrochemical properties of graphites.[31] Structure analysis revealed that the average interlayer spacing and lattice parameters decreased upon addition of boron, suggesting that boron replaced carbon in the layers. The final point was highlighted as the principle cause for the improvement in electrochemical properties. It was found that the properties were independent of the boron source used during the synthesis.

6 Cathodes

$LiMn_2O_4$ and related materials

The effect of the metal ion source on the properties of $LiMn_2O_4$ has been investigated using a tartaric acid gel process by Hon.[32] When metal nitrates were used as the source, the prepared samples were found to contain Li_2MnO_3 and Mn_2O_3 impurities, whereas single phase samples could be prepared from the acetates. The capacity of a single phase $LiMn_2O_4$ sample prepared at 500 °C from acetates was 117 mAh g^{-1}, which not surprisingly was higher than the corresponding nitrate derived sample. This highlights the need for careful selection of starting materials.

Tang *et al.* have prepared uniform single crystals of $LiMn_2O_4$ spinel using a LiCl flux method.[33] The effects of reaction times and temperature on the composition, size and morphology were examined, with temperature found to be the most critical parameter. Stoichiometric crystals were grown at 850 °C, whereas lithium rich and lithium deficient crystals were found at lower and higher temperatures respectively. Crystals of composition $Li_{1.18}Mn_2O_{4.28}$ with a plate-like morphology and thickness of less than 0.1 μm had discharge capacities of 112 mAh g^{-1} with good cycling properties.

Monge and coworkers have also prepared single crystals of $LiMn_2O_4$.[34] by electrocrystallization methods. A series of different crystals were grown by systemically varying the flux, time, temperature, voltage and current, with crystals ranging in size from 0.1 to 1 mm. It was found that both lithium (94%) and manganese (6%) occupied the *8a* site within the spinel structure; with the *32e* oxygen site occupancy refining to unity. These crystals were electrochemically cycled and it was found that Mn migrated from the octahedral to tetrahedral site. The majority of the structural changes associated with cycling were found to be nearly reversible, but some of the Mn was found to remain on the tetrahedral *8a* site. These results indicate that changes occur at the atomic level during cycling as well as at the macroscopic level.

Singh *et al.* have prepared $LiMn_2O_4$ thin films using pulsed laser deposition (PLD) and UV assisted pulsed laser deposition (UVPLD), and examined the microstructural and electrochemical properties of the prepared films.[35] It was noted that the UV assisted method produced samples with higher crystallinity and smaller lattice constants. This was attributed to the samples being oxygen rich defective spinels. First charge capacities of 115 and 97 mAh g^{-1} were observed for the PLD and UVPLD films respectively.

Julien and coworkers have prepared Cr and Cu doped samples of $LiMn_2O_4$ using wet chemistry methods.[36] Samples of $LiMn_{2-y}Cr_{y/2}Cu_{y/2}O_4$ were synthesised using aqueous solutions of metal acetates and succinic acid. The samples were characterised by X-ray powder diffraction, Raman- and FTIR-spectroscopy. Reversible capacities of the order of 100 mAh g^{-1}, with a 95% capacity retention over 40 cycles, were observed for the $y = 0.1$ composition. The improvement in the cycling stability was explained in terms of the Mn^{3+}/Mn^{4+} ratio in the doped samples.

Hernan *et al*. have prepared a series of spinels of composition $LiM_xMn_{2-x}O_4$ (M is Fe, Co or Ni, x ~0.3) using a carbonate based precursor method followed by heating in air at 400, 600 and 900 °C.[37] The samples were characterised by chemical analysis, X-ray powder diffraction and X-ray Photoelectron Spectroscopy (XPS). XPS measurements indicated that Co^{3+} and Fe^{3+} oxidation states were favoured, whereas a 2+ state was observed for the Ni samples. No evidence of Mn^{2+} was found. For the sample prepared above 400 °C, small amounts of the transition metal elements were detected on the *8a* site. Electrochemical measurements indicated that all of the materials prepared had the ability to extract lithium at voltages above 4.5 V, with oxidation of the dopant transition metal observed. However, the reversibility of this process was improved as the sintering temperature was increased. This was thought to be due to the improved crystallinity and smoother particle surfaces of the samples. The situation was found to be different for the Fe doped samples which had a capacity of ~100 mAh g^{-1} with good cycling properties. However, the samples prepared at 900 °C were found to have a severe degradation in cycling properties with no capacity

after the first few cycles. This was explained in terms of Fe_2O_3 extrusion as well as changes in the sample morphology. The Co and Ni samples prepared at 900 °C were found to deliver capacities of 100 and 120 mAh g^{-1} at voltages of 4.5 V.

Shigemura has also examined Fe and Co doped spinels for applications in 5 V cells.[38] Samples of Li $(Fe,Co)_xMn_{2-x}O_4$ ($0 \leq x \leq 0.5$ for Fe, $0 \leq x \leq 1.0$ for Co) were prepared by solid state reaction at temperatures between 750 and 800 °C in a flowing O_2 atmosphere. The structures were determined by Rietveld analysis using neutron diffraction data and showed the presence of Fe and Co on the Li *8a* site. XAFS measurements indicated that the Fe–O distance was longer, while the Co–O distance was shorter, when compared to the average $M_{16d}O_{32e}$ distances calculated from the structure refinement. This suggests a distortion away from local cubic symmetry. Detailed electrochemical charge/discharge data is presented in the article.

Liu *et al*. have attempted to improve the high temperature performance of $LiMn_2O_4$ by micro-emulsion coating with $LiCoO_2$.[39] The electrochemical performance was evaluated at 55 °C, with the authors reporting an improvement in the high temperature performance, with a small reduction in capacity. At room temperature the stability of the materials was reported to be good.

Tang and co-workers have investigated the effects of yttrium doping.[40] X-Ray powder diffraction indicated that the solubility limit for Y was ≤0.02 (in $LiMn_{2-x}Y_xO_4$). Electrochemical analysis of the materials gave a first discharge capacity of 118 mAh g^{-1} with 98% capacity retention after 100 cycles using a charge/discharge rate of 0.2 C. This suggests that Y doping is beneficial to the properties of this material.

Han *et al*. have prepared iodine-containing lithium manganese oxide spinels and evaluated the electrochemical performance of two different materials.[41] Iodine-containing cation deficient spinel was prepared by reaction of Li and MnO_2 with a nominal composition of $Li_{0.99}Mn_{1.98}O_4I_{0.02}$ obtained at 800 °C. A lithium rich sample was prepared by reaction of $LiMn_2O_4$ with LiI yielding a nominal composition of $Li_{1.01}Mn_{1.99}O_4I_{0.02}$. The cation deficient sample was found to give capacities of 113 mAh g^{-1} with good cyclability and rate capacity in the 4 V regions. Better results were obtained for the lithium rich sample with initial discharge capacities of the order of 124 mAh g^{-1} being observed along with 96% capacity retention after 20 cycles.

$LiMnO_2$

Armstrong *et al*. have continued work on L–$LiMnO_2$* with a study on nonstoichiometric $Li_xMn_yO_2$.[42] L–$Li_xMn_yO_2$ has been prepared from $NaMnO_2$ using ion exchange methods. The authors have examined the effects of varying the synthesis conditions of the precursor as well as the ion exchange mechanism, and found that significant differences in the number of vacancies could be induced. Differences were noted by powder X-ray diffraction in the lattice parameters and the *hkl* dependent peak broadening. These differences were examined using Rietveld analysis of powder neutron diffraction data. The electrochemical properties were found to be very sensitive to the composition and the defect structure, with capacity in the region of

* L–$LiMnO_2$ denotes layered material, O–$LiMnO_2$ denotes orthorhombic material.

190–200 mAh g^{-1} observed at a C/7 discharge rate. Long range cycling of the material showed a capacity fade of 0.12% at room temperature, which is superior to that seen for undoped $LiMnO_2$. All of the materials examined during this work were found to convert to a spinel like material. Guo have prepared L–$LiMn_{1-x}Cr_xO_2$ using the Pechini method and examined the effects of ethylene glycol content and calcination temperature on the structure and electrochemical performance.[43] It was noted that, as the molar ratio of ethylene glycol to citric acid was increased, the sample homogeneity improved. Traces of MnO were detected in materials heated below 800 °C for 4 hours. A comparison with samples prepared by solid state reaction showed an improvement in the charge/discharge capacities, with discharge capacities of ~150–160 mAh g^{-1} observed for the samples prepared by the Pechini method (140 mAh g^{-1} by solid state methods). The improvement is thought to be due to the smaller particle size and better sample homogeneity.

Hwang and co-workers have examined the local structure of L–$LiMnO_2$ using X-ray Absorption and micro-Raman Spectroscopy. The experiments were performed to probe the changes in the local structure during the delithiation and relithiation process.[44] The results of these experiments indicated a change in the local structure around the Mn from a layered to a spinel-like environment. The authors prepared $LiMn_{1-x}Cr_xO_2$ ($0 < x < 0.15$) and, as expected, an improvement was noted in the electrochemical properties of the Cr doped materials. XAS and micro-Raman spectroscopy indicated that the Cr ions were fixed on the octahedral sites before and after the electrochemical measurements, and that Mn was stabilized through a shortening of the Mn–O bond lengths. These features are thought to be the sources of the electrochemical capacity improvement of the Cr doped samples over undoped materials. Discharge capacities of the doped material were of the order 165 mAh g^{-1} compared to 125 mAh g^{-1} for the undoped material.

Hydrothermal synthesis has been used by Myung *et al.* to prepare O–$LiMnO_2$[45,46] and Co-doped samples.[47] Well-ordered samples were prepared from Mn_3O_4 (or $(Co_xMn_{1-x})_3O_4$ in the case of Co doped samples) and excess aqueous solutions of LiOH at 170 °C. The electrochemical properties were described as good, with better results observed for the Co doped samples. The same authors have also examined the use of emulsion drying to prepare single phase O–$LiMnO_2$ and examined the cycling properties.[48] The emulsion-dried precursor was first heated at low temperature, followed by a second heating at 925 °C under an argon atmosphere. The resultant material was structurally characterised using TEM and electron diffraction methods. Charge/discharge measurements gave capacities of the order of 170 mAh g^{-1}, with >155 mAh g^{-1} observed after 300 cycles.

The effects of sample grinding of O-$LiMnO_2$ has been examined by Lee.[49] A highly crystalline sample of O–$LiMnO_2$ was prepared from LiOH and MnOOH at 1000 °C in an argon atmosphere followed by quenching to room temperature. The samples had poor discharge capacities of 34 mAh g^{-1} at room temperature. The "as prepared samples" were then ground for 24 hours and the electrochemical properties re-examined; discharge capacities of 210 mAh g^{-1} and capacity retention of 96% in the 3–4 V region over 50 cycles was observed.

Cho *et al.* have prepared samples of O–$LiMnO_2$ coated with either Al or Co and examined the electrochemical properties of these materials at 55 °C.[50,51] In the first of these papers the authors reported the Al_2O_3 coating of the pre-prepared materials at

temperatures in the range of 150–700 °C. For the samples prepared at 600–700 °C a uniform distribution of Al through the particles was reported, whereas the samples prepared at 400–500 °C showed that the Al was mostly concentrated at the surface of the particles. Significant differences were noted between the low and high temperature coating treatments, with significantly better results seen for the 400–500 °C samples. The best sample was that obtained at 400 °C, which after the initial "conditioning cycles", had discharge capacities of greater than 160 mAh g^{-1} with little capacity fade over 50 cycles. Samples prepared at 600–700 °C had initial capacities in the region of 100 mAh g^{-1} and 40% capacity face over 50 cycles. For Co doped samples the initial capacity was found to be better with discharge capacities of the order of 180 mAh g^{-1} being seen after the "conditioning cycles", although this was seen to drop to 160 mAh g^{-1} after 50 scans.

$LiCoO_2$

Chang *et al*. have prepared $LiCoO_2$ materials by refluxing methods.[52] The authors found that by controlling the oxidation potential of the reaction environment samples could be prepared from $Co(OH)_2$ at temperatures as low as 130 °C, with the alkaline solutions and O_2 flow inducing the reaction of the Co^{2+} in the $Co(OH)_2$. X-ray powder diffraction showed the samples to be well crystallised with a layered structure. Initial electrochemical capacities were found to be of the order of 130 mAh g^{-1} on initial discharge, however the results of extended cycling showed capacity fading. Burukhin has also examined the hydrothermal synthesis of $LiCoO_2$.[53] The samples were prepared from aqueous solutions of $Co(NO_3)_2$, LiOH and H_2O_2 using a range of different Co:Li and Co:H_2O_2 ratios at temperatures in the range of 150–250 °C, and with times ranging from 30 minutes to 24 hours. Samples with the high temperature $LiCoO_2$ structure were observed by X-ray diffraction, scanning- and transmission-electron microscopy. Samples prepared with higher LiOH concentrations showed better crystallinity. Discharge capacities of the order of 130 mAh g^{-1} with 3.1 mAh g^{-1} fade per cycle were observed for samples prepared with no additional heat treatment. Annealing of the hydrothermally prepared samples at 230 °C gave samples with a discharge capacity of 120 mAh g^{-1} and capacity fade of 1.6 mAh g^{-1} per cycle.

Mechanical alloying of hydroxides has been used to prepare samples of $LiCoO_2$.[54] High temperature $LiCoO_2$ was prepared by mechanically alloying $LiOH{\cdot}H_2O$ and $Co(OH)_2$ followed by firing at different temperatures. A number of sintering temperatures were examined with a discharge capacity of 152 mAh g^{-1} obtained for the sample prepared at 600 °C, albeit with poor cycling performance. When a sintering temperature of 850 °C was used the capacity was slightly lower (142 mAh g^{-1}), although a higher capacity retention of 93% after 30 cycles was observed.

Kushida and Kuriyama have examined the sol–gel growth of $LiCoO_2$ onto silicon substrates using a spin coating method.[55] The raw materials, lithium and cobalt acetates were mixed in a 1:1 ratio and dissolved in methanol, together with citric acid, which acts as the chelating agent. The stoichiometry of the final product was found to be highly sensitive to the ratio of the two starting materials. The raw materials were spin coated onto a Si substrate and annealed at temperatures in the range 300–800 °C for 30 minutes under a O_2 flow. Characterisation was performed using X-ray

diffraction and Raman scattering. The results indicated a structural transformation from the spinel to the layered rock salt structure in the region of 600 °C. The authors presented no electrochemical data for these materials.

Similar to last year a number of groups have been investigating methods of preparing thin films of $LiCoO_2$.[56,57] Pracharova *et al.* have used radio frequency sputtering methods to grow films on silicon substrates coated with gold. X-ray powder diffraction and Raman spectroscopy indicated the formation of the HT hexagonal phase when an annealing temperature of 500 °C was used. However, the films prepared at temperatures less than 200 °C were found to have better properties.

Bouwman *et al.* have deposited $LiCoO_2$ films onto silicon and steel substrates using RF sputtering and pulsed laser deposition.[58] Both films showed preferred orientation, which was perpendicular for the RF deposited films and parallel to the *c* axis for the PVD films. The lithium intercalation rates were found to be strongly dependent on this alignment of the films.

Commercial $LiCoO_2$ has been coated with different metal oxides including MgO, SnO_2 and Al_2O_3, and the electrochemical properties examined.[59,60] The sample morphology and structure was examined using scanning electron and high resolution transmission electron microscopy. The coating layers were amorphous and compact for all the coating materials examined. The different coatings were found to drastically affect the electrochemical stability of the $LiCoO_2$, with MgO found to be the most stable and SnO_2 the least stable. Cyclic voltammetry and charge/discharge experiments indicated that these modifications affect the phase transition below 4.5 V, and suppress the phase transition at 4.58 V. Capacities of 190 mAh g^{-1} were observed for all samples on initial discharge. However, the Al_2O_3 and MgO stabilised the long term cycling properties of these materials. Capacities of about 180 mAh g^{-1} were seen for the MgO coated sample with exceptional stability seen for the first 20 cycles. Capacities of 210 mAh g^{-1} were observed when the upper voltage cut off was set to 4.7 V.

Fujiwara and co-workers have developed a novel method for preparing crystalline $LiCoO_2$ films on paper.[61] The authors have developed a novel method that enables direct fabrication of $LiCoO_2$ onto porous films using low temperature electrodeposition methods. The films were prepared from LiOH and $CoSO_4$ solutions at 120 °C using a current of approximately 1 mA cm^{-2}. It was noted that the film did not cover the entire substrate, but formed in the shape of the carbon anodes used during the deposition process.

$LiNiO_2$

Song and Lee have investigated $LiNiO_2$ prepared by sol–gel methods and examined their electrochemical properties.[62] Single phase lithium nickelate has been prepared from $LiNO_3$ and $Ni(NO_3)_2{\cdot}6H_2O$ with citric acid used as the chelating agent. The optimum conditions were found to be 600 °C in air for 5 hours followed by 13 hours at 800 °C in a flowing oxygen atmosphere. The prepared materials were found to be of a relatively uniform morphology with a particle size range of 3–5 μm. The electrochemical properties were found to be relatively good with an initial discharge capacity of 168 mAh g^{-1} and slightly less than 93% capacity retention after 20 cycles.

Chang *et al.* have investigated the effects of crystallite size on the electrochemical properties of $LiNiO_2$.[63] A sample of $LiNiO_2$ with ~1% disorder on the lithium site was prepared using particulate sol–gel methods, and was found to have an initial high capacity of 205 mAh g^{-1} at a C/2 discharge rate. When the particle size increased from 0.3 to 0.8 μm a 10% decrease in observed capacity was seen. However, further analysis showed that Li *3a* site defects and impurity phases influence the electrochemical properties to a greater extent than particle size.

Kim *et al.* have reported the fabrication of a thin film $LiNiO_2$ cathode using RF magnetron reactive sputtering.[64] The film was grown from a synthesised $LiNiO_2$ target in a mixed oxygen/argon atmosphere and then rapidly annealed at 700 °C for 10 minutes in an oxygen atmosphere. Relatively good capacities and reversibility were found for materials prepared in this manner.

Arai *et al.* have examined the thermal reactions of delithiated lithium nickelates and electrolyte solutions.[65] The thermal stability was evaluated in a number of electrolyte solutions such as ethylene carbonate, dimethyl carbonate, $LiPF_6$, and the exothermic heat liberated measured by DSC and compared to the results obtained for $LiCoO_2$. The same group has also examined chemically derived Li_xNiO_2 ($x \sim 0$) polymorphs as potential insertion anodes.[66] Five polymorphs of NiO_2 have been prepared by treating $LiNiO_2$ with H_2SO_4, with some of the samples being heated at low temperatures. $Li_{0.10}NiO_2$ with two layered phases was found to transform to a single layered phase at 160 °C and then to a spinel related phase at 170 °C. A sample of $Li_{0.04}NiO_2$ with a CdI_2 structure also converted to a spinel phase on heating. Examination of the Ni–O bond distances indicated that the nickel oxidation state was always approximately 4+.

Moshtev *et al.* have presented a simple method for the synthesis of $LiNi_{1-y}Co_yO_2$ (y = 0.2 to 0.3).[67] Precursors were obtained by a solution method, which was then reacted with LiOH. Electrochemical measurements were then performed using a C/2 rate between 4.3 and 2.8 V. The discharge capacity of the cathodes, not surprisingly was found to be dependent on the value of y with values of 190–176 mAh g^{-1} observed after 10 cycles and 160–165 after 60 cycles.

Samples of layered Li–Mn–Ni–O_2 have been prepared by heating metal acetates with the preparation of all members of the solid solution between $LiNiO_2$ and Li_2MnO_3 being successful.[68] It was found that the degree of cation disorder as well as the capacity was closely related to the ratio of Li, Mn and Ni in the formula. Chronopotentiograms as well as *ex-situ* XRD measurements indicated that the complex series of phase transitions associated with $LiNiO_2$ were strongly suppressed when the Mn/(Mn + Ni) ratio was 0.1 and 0.2, and completely suppressed when the ratio was 0.5.

Chitrakar and co-workers have prepared single-phase materials of layered $LiNi_{0.5}Mn_{0.5}O_2$ and cubic rock salt $Li_{0.4}Ni_{0.3}Mn_{0.3}O$.[69] The samples were prepared from $NiMnO_3$ and $LiOH{\cdot}H_2O$, with the layered sample being prepared at 1000 °C in air and the cubic sample at 700 °C under nitrogen. The cubic phase could be converted to a $LiNiO_2$ type material on heating in air at 400 °C.

Shin and co-workers have prepared samples of $Li[Li_{(1-2x)/3}Ni_xMn_{(2-x)/3}]O_2$ and examined the electrochemical properties.[70] Samples with x values of 0.41, 0.35, 0.275 and 0.2 were prepared using sol–gel methods. It was found that the discharge capacity increased with increasing lithium content on the *3a* site. A cathode prepared from $Li(Li_{0.2}Ni_{0.2}Mn_{0.6})O_2$ had discharge capacities of 200 and 240 mAh g^{-1} with good cyclability at 30 and 55 °C respectively.

Kang *et al*. have examined the effects of doping Co, Al, and Ti in $Li(Ni_{0.5-x}Mn_{0.5-x}M_{2x})O_2$ where $x = 0$ and 0.025.[71] The parent material $Li(Ni_{0.5}Mn_{0.5})O_2$ had a discharge capacity in the region of 120 mAh g^{-1} with 0.09% capacity fade per cycle over 40 cycles (limits set at 2.8 to 4.3 V). Doping with Co, Al and Ti gave capacities of 140, 142, and 132 mAh g^{-1} respectively with almost no capacity fading. Impedance measurements on the materials indicated that Co improved the electronic conductivity, little difference was seen between the undoped and the Ti doped sample, with Al reducing the electronic conductivity. No transformation from a layered structure to a spinel-like structure was observed during the electrochemical cycling.

7 Li ion conductors

Polymeric materials

Ulrich *et al*. have examined a solid hybrid polymer (SHyP) electrolyte network and its suitability for utilization in lithium batteries.[72] The material was prepared by hydrolyzing (3-glycidyloxypropyl)trimethoxysiliane and aluminium *sec*-butoxide in 0.01 N HCl. The resultant material was then blended with polyethyleneoxide (PEO) and lithium triflate. The electrolyte showed no evidence of PEO crystallinity and was found to have high ionic conductivity, high transference number and good mechanical strength.

Li and co-workers have evaluated a polyethylene oxide–$BaTiO_3$ composite material as a possible polymer electrolyte in a 4-volt polymer battery.[73] The lithium salt used was $LiN(CF_3SO_2)_2$-$LiPF_6$ (90:10) and when used with Li/[PEO-($LiN(CF_3SO_2)_2$-10 wt.% $LiPF_6$)]-10 wt.% $BaTiO_3/LiNi_{0.8}Co_{0.2}O_2$/Al good cycling properties were observed. Capacity fading of 0.28% per cycle was observed for cells examined at 80 °C.

A UV-cured gel polymer electrolyte based on polyethylene glycol diacrylate (PEGDA) oligomer and polyvinylidene fluoride (PVdF) has been prepared and the physical and electrochemical properties in cells evaluated.[74] These films were found to have good mechanical and electrochemical stability with conductivities of 4 S cm^{-1} at room temperature. When examined in a Li/Polymer/$LiCoO_2$ cell, capacity retention was found to be good.

Xu and Angell have prepared and characterised novel polyMOB solid electrolytes.[75] The synthesis of chain polymers with monooxalato orthoborate (MOB) moieties with controlled anionic separation was described. Conductivities of 10^{-5} S cm^{-1} were observed at room temperature for a solid polymer with fourteen ethyleneoxy repeating units. The electrochemical stability window was found to be greater than 4.5 V.

Polymer gel electrolytes supported with microporous polyolefin membranes have been examined by Wang *et al*.[76] The polymer gel electrolyte was prepared using poly(vinylidiene fluoride-*co*-hexafluropropylene), lithium salt and a carbonate solvent. Ionic conductivities of 10^{-3} S cm^{-1} were observed at room temperature with the gel stable up to 5 V. The electrolyte was found to have good mechanical properties and was stable during repeated cycling.

A composite polymer electrolyte film made from polyurethane and polyacrylonitrile has been prepared by two different processes by Kuo and co-workers.[77] Sample

morphology was examined by SEM, which revealed differences in the morphology depending on the method of preparation. The conductivity at room temperature was found to be 10^{-4} S cm^{-1}, with the electrochemical stability window extending from 2.5 to 4.5 V. Thermogravimetric analysis indicated that the samples have good thermal stability, with a decomposition temperature greater than 300 °C.

8 Non-polymer systems

Murayama *et al.* has continued to examine Thio-LISICON materials.[78] A new series of thio-LISICONS has been found in the ternary system Li_2S–SiS_2–Al_2S_3 and Li_2S–SiS_2–P_2S_5. The structure of the new materials $Li_{4+x}Si_{1-x}Al_xS_4$ and $Li_{4-x}Si_{1-x}P_xS_4$ were determined by X-ray Rietveld analysis, and the electrochemical properties examined using a variety of methods. The structure of the parent material, Li_4SiS_4 is related to the γ-Li_3PO_4 type structure. It was noted that when Li^+ interstitials or Li^+ vacancies were created by partial substitution of Al^{3+}, Si^{4+} or P^{5+} a noticeable increase in ionic conductivity was observed. The highest conductivity was observed in the $Li_{3.4}Si_{0.4}P_{0.6}S_4$ composition, which has a conductivity of 6.4×10^{-4} S cm^{-1} at 27 °C. It was also noted that this solid solution series is stable in the range of 5 V *vs.* Li at room temperature. In addition to the above work, the same group has determined the structure of Li_4GeS_4 from refinement of X-ray and neutron diffraction data.[79] The structure is closely related to that of γ-Li_3PO_4 consisting of a hexagonal close-packed array of sulfide ions, with Ge in the tetrahedral sites of the framework. Li ions were shown to occupy both octahedral and tetrahedral sites, and the authors discussed possible Li diffusion pathways. The structure is presented in Fig. 2.

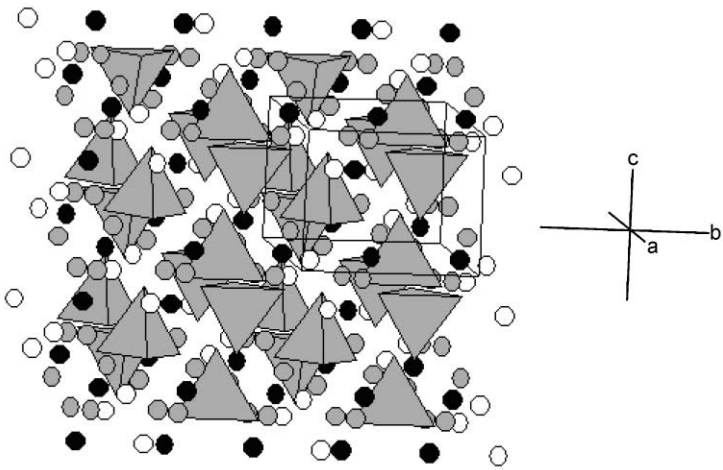

Fig. 2 Structure of Li_4GeS_4 obtained from Rietveld refinement using Neutron data. Li1 shown as white spheres, Li2 shown as light grey spheres, Li3 shown as black spheres. GeS_4 shown as grey tetrahedra.

Research on Li ion conduction in NAISCON-type materials has continued to attract attention. Arbi *et al.* have analysed the phase transition from triclinic to rhombohedral symmetry in $LiZr_2(PO_4)_3$ using DSC, XRD, and NMR (^{31}P and ^{7}Li).[80] Four-fold coordination of Li was confirmed in the triclinic phase. Above the phase transition (310 K), delocalisation of Li over structural sites along the conduction path were observed, which explains the high Li ion conductivity in this system. The same group has examined the conductivities of the systems $Li_{1+x}Ti_{1-x}Al_x(PO_4)_3$ ($0 \leq x \leq 0.7$).[81] Al substitution was shown to enhance grain boundary conduction, and new broad peaks detected by NMR support the conclusion of the formation of an amorphous Li ion conducting phase, which accounts for the overall increase in conductivity. In the case of samples with $x > 0.5$, $Li_4P_2O_7$ appeared as a secondary phase, and there was an overall decrease in conductivity.

In terms of other systems, perovskite materials are also being investigated by a number of groups. Inaguma *et al.* have examined the structure of the perovskite $La_{2/3-x}Li_{3x}TiO_3$ at room temperature and 77 K.[82] The Li ions were located off centre in two equivalent positions within the A sites. The authors suggest that Li ion conduction in this compound occurs in the vicinity of La-poor layers, meaning that the conductivity is 2 dimensional rather than 3 dimensional. In terms of doping studies, Nakayama *et al.* have examined the Li ion conductivity of the perovskite systems, $(La_{0.3}Li_{0.1})_yM_x$-$Nb_{1-x}O_3$ (M = Zr, Ti, Ta).[83] All dopants resulted in a reduction in Li ion conductivity contrary to the authors' expectations. In addition, Morata-Orrantia *et al.* have examined the conductivity of the solid solution $La_{2/3}Li_xTi_{1-x}Al_xO_3$ ($0.06 \leq x \leq 0.3$).[84] The Li ion conductivity was shown to increase with increasing Li content up to a value of 7.6×10^{-5} S cm^{-1} at room temperature for $x = 0.25$.

High Li ion conduction has been observed in the compound $LiMgFSO_4$ ($\sigma_{793\ K} = 1.5 \times 10^{-3}$ S cm^{-1}, $E_a = 0.94$ eV).[85] The structure consists of a framework containing MgO_4F_2 octahedra and SO_4 tetrahedra, with the Li disordered between two cavity sites within the framework.

9 Oxide ion conductors/solid oxide fuel cells

As in previous years, there has been a considerable amount of research on oxide ion conductors, which has been driven by their potential for use as the electrolyte in a solid oxide fuel cell (SOFC). At present, the favoured electrolyte for manufacturers of SOFCs is yttria stabilised zirconia (YSZ), although over the last few years, interest in other potential electrolytes has grown significantly. This interest in alternative electrolytes is being driven by the academic community, which has not only developed the electrolytes but also demonstrated their performance in single cell SOFCs. A decade ago, the main focus of research on oxide ion conductors was materials with the fluorite-type structure. At present, fluorite-type materials still attract interest, but now other structure-types are gaining considerable attention, particularly perovskite systems.

In terms of fluorite-type materials, there is still interest in doped zirconia, although academic research is moving towards doping zirconia with scandia rather than yttria. This has been driven by the higher oxide ion conductivity of scandia stabilised zirconia (SSZ), along with reductions in the price of Sc_2O_3. The higher oxide ion

conductivity allows the potential for operation at lower temperatures, thus reducing problems associated with cell sealing. Kosacki *et al*. have performed detailed measurements of the conductivity of this system, and determined the electronic and ionic contribution to the conductivity.[86] Their results show that the microstructure plays a significant role in determining the properties, with the electronic conductivity being enhanced in nanocrystalline samples, such that it dominates the total conductivity in reducing atmospheres.

Single cell SOFCs have been constructed using this electrolyte and the properties tested.[87,88] Cells were constructed using a Ni–SSZ cermet as a support with a thin electrolyte of SSZ applied using either dip coating or electrophoretic deposition. A Pt–SSZ cermet was used as the cathode, and it was shown that this contributed 80% of the resistance of the cell and hence was responsible for the biggest degradation of the cell performance. Use of $La_{1-x}Sr_xCoO_3$ as the cathode to improve performance was unsuccessful due to the formation of an insulating layer with SSZ. Work is ongoing trying to improve the cathode performance.

Mixed yttria and scandia doped systems have also been examined. After obtaining promising results for $Y_{0.2}Zr_{0.62}Ti_{0.18}O_{1.9}$ as an SOFC anode material, Tao and Irvine have studied similar systems with Sc doping to improve the oxide ion conductivity.[89] The highest ionic conductivity (0.01 S cm^{-1} at 900 °C) and electronic conductivity (0.14 S cm^{-1} at the same temperature) were observed for $Sc_{0.2}Zr_{0.62}Ti_{0.18}O_{1.9}$ and $Sc_{0.1}Y_{0.1}Zr_{0.6}Ti_{0.2}O_{1.9}$ respectively. The best potential anode composition in terms of a balance between the two was the composition $Sc_{0.15}Y_{0.05}Zr_{0.62}Ti_{0.18}O_{1.9}$, with ionic and electronic conductivities at 900 °C of 7.8×10^{-3} and 0.14 S cm^{-1} respectively.

In terms of other fluorite-type systems, research on rare earth doped ceria has gained in stature, with again the prospect of lower temperature operation using this electrolyte. Dikmen *et al*. have prepared $Ce_{1-x}Gd_xO_{2-y}$ solid solutions *via* a hydrothermal method.[90] The method produces uniformly small particle sizes (41–68 nm), which then allows sintering to give dense pellets at temperatures up to 300 °C lower than temperatures for conventional ceramic powders.

Kim *et al*. have examined the performance in an SOFC of a YSZ/YDC (yttria doped ceria) composite electrolyte, prepared by sol–gel coating a YSZ film 2 μm thick on a YDC substrate 1.6 mm thick.[91] Improved performance was observed compared to the uncoated electrolyte, which was attributed to the YSZ acting as an electron blocking layer.

Bismuth-based oxide ion conductors have also continued to interest researchers. These materials tend to show the highest oxide ion conductivities of any ceramics, but suffer from the fact that Bi is readily reducible and so this introduces electronic conductivity under reducing conditions. To counteract this problem, Wachsman has investigated bilayer electrolytes so that the Bi based electrolyte only experiences oxidising conditions.[92] In the experiments $(Er_2O_3)_{0.2}(Bi_2O_3)_{0.3}$ was used on the high $p(O_2)$ side while $(Sm_2O_3)_{0.1}(CeO_2)_{0.9}$ was used on the low $p(O_2)$ side, and the results showed that these bilayer electrolytes have significant potential for technological applications, such as SOFCs and oxygen separation membranes.

In terms of attempts to optimize the oxide ion conductivity in Bi-based fluorite-type materials, W doping has shown promising results.[93] Conductivities of 0.57 S cm^{-1} (1073 K) and 0.043 S cm^{-1} (773 K) were observed for $(Bi_2O_3)_{0.44}(Dy_2O_3)_{0.04}(WO_3)_{0.04}$, which represent the highest values reported for an oxide ion conducting solid

electrolyte. In other studies of Bi-based systems, Uma *et al*. have examined the oxide ion conductivity of the scheelite related phases $Bi_{1-2x}A_{2x}VO_{4-x}$ (A = Ca, Sr, Cd; $0 \leq x \leq 0.25$).[94] Conductivities as high as those for stabilised zirconias have been obtained for these phases. Grins *et al*. have reported a new phase $Bi_6Cr_2O_{15}$, whose structure consists of $(Bi_{12}O_{14})_n^{8n+}$ columns surrounded by CrO_4^{2-} tetrahedra.[95] A conductivity of 3.5×10^{-5} S cm^{-1} at 600 °C was obtained for this phase.

In terms of the so-called BIMEVOX systems ($Bi_4V_{2-x}M_xO_{11-y}$: M = transition metal), Watanabe *et al.* have reported further results on the time dependant degradation of the conductivity in these ionic conductors.[96] The results show that the process is more complicated than initially thought, with the authors showing a transition to a new phase with the α-$Bi_4V_2O_{11}$ structure on prolonged annealing at 450 °C for several hundred hours. Abrahams and Krok have reviewed the defect structures of BIMEVOX systems, and devised two general defect equations for solid solution formation.[97] In the first model (equatorial vacancy) vacancies are located at bridging sites within the V layers, while in the second model (apical vacancy), vacancies are located in non-bridging apical sites within these layers. The authors show that in most cases the equatorial vacancy model yields theoretical solid solution limits close to those observed, and discuss the mechanism for oxide ion migration in respect of these models.

After fluorite-type materials, perovskite-type materials have attracted the most interest, with doped $LaGaO_3$ ($La_{1-x}Sr_xGa_{1-y}Mg_yO_{3-z}$ (LSGM)) (Fig. 3) appearing to be a very promising SOFC electrolyte. Yamaji *et al* have compared the conductivities of the phases $La_{0.9}Sr_{0.1}Ga_{0.8}Mg_{0.2}O_{2.85}$ and $La_{0.9}Ba_{0.1}Ga_{0.8}Mg_{0.2}O_{2.85}$.[98] Both phases had similar total conductivities as well as similar electronic conductivities. In cell operation with these electrolytes, the Sr doped sample performed better, which was attributed to the higher stability of this system. The cell with $La_{0.9}Ba_{0.1}$-

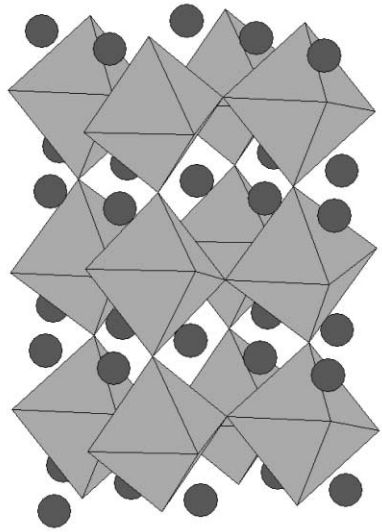

Fig. 3 The structure of $La_{0.9}Sr_{0.1}Ga_{0.8}Mg_{0.2}O_{2.85}$ (dark spheres = La/Sr; octahedra = Ga/MgO_6).

$Ga_{0.8}Mg_{0.2}O_{2.85}$ showed a rapid increase in anode overvoltage with operating time suggesting degradation of the electrolyte.

Jang *et al*. have examined the partial electronic conductivities of the phases $La_{0.9}Sr_{0.1}Ga_{0.9}Mg_{0.1}O_{2.9}$, $La_{0.9}Sr_{0.1}Ga_{0.8}Mg_{0.2}O_{2.85}$ and $La_{0.8}Sr_{0.2}Ga_{0.8}Mg_{0.2}O_{2.8}$ between 700 and 900 °C.[99] With increasing Sr and Mg content, the hole and electron conductivities were both shown to decrease. The electronic transference numbers were found to be in the range 10^{-2}–10^{-3}.

The reactivity of LSGM electrolytes with other components of a SOFC ($La_{1-x}Sr_xMnO_3$, $La_{1-x}Ca_xCrO_3$, and Ni) has been investigated in the range 650–1000 °C.[100] Reaction was shown to occur, with phases such as $LaSrGa_3O_7$, $LaSrGaO_4$, $La_4Ga_2O_9$, and $Ca_2Ga_2O_5$ being observed, which could cause problems in cell operation.

A number of groups have examined the performance of LSGM based SOFCs. Fukui *et al*. have prepared a SOFC employing a thin LSGM electrolyte film to investigate possible use at intermediate temperatures.[101] The thin film of LSGM was fabricated using a tape casting method, achieving a relative density of over 99%, along with a conductivity of 0.054 S cm^{-1} at 700 °C. Ni–scandia doped ceria and $La_{1-x}Sr_xCoO_3$ were used as anode and cathode respectively and the resultant single cell gave very good performance with a power density of over 0.4 W cm^{-2} at 700 °C. Yan *et al.* have also examined thin film LSGM based SOFCs.[102] In their cell Ni–YSZ was used as the anode, with a $La_{1-x}Sr_xMnO_3$ (LSM)-YSZ composite as the cathode. The thin film electrolyte was ≈15μm thick. To avoid reaction with Ni in the cermet on sintering the film, the NiO was impregnated into the porous YSZ anode support after depositing and sintering the LSGM thin film. A maximum power density of 0.85 W cm^{-2} at 800 °C was achieved with H_2 as the fuel and air as the oxidant.

In terms of optimizing the performance of these LSGM based SOFCs, Ishihara *et al*. have investigated the optimum electrodes to use. La-doped $BaCoO_3$ has been investigated as the cathode.[103,104] The electrical conductivity of $Ba_{1-x}La_xCoO_3$ increased systematically with increasing amounts of La leading to a decrease in cathode overpotential. The optimum composition was shown to be $Ba_{0.6}La_{0.4}CoO_{3-x}$, and using this material as a cathode resulted in slightly higher power densities (120 mW cm^{-2}) than for using a $Sm_{0.5}Sr_{0.5}CoO_3$ cathode.

Doped $LaGaO_3$ has also been investigated for possible use in other applications. Ishihara *et al*. have shown that the composition $La_{0.7}Sr_{0.3}Ga_{0.6}Fe_{0.4}O_3$ exhibits high oxygen permeation rates and represents a promising oxygen separation membrane/membrane reactor material.[105,106]

The use of LSGM in a composite cathode for YSZ based SOFCs was examined by Armstrong *et al*.[107] The cathode used was a composite of $La_{0.8}Sr_{0.2}MnO_3$ and $La_{0.9}Sr_{0.1}Ga_{0.8}Mg_{0.2}O_{2.85}$ with the proportions varying between 70–30 wt% and 30–70 wt %. The lowest cathode overpotential was observed for the composite with 50–50 wt %. A cell with this cathode fired at 1150 °C exhibited an area specific resistance of 0.18 Ω cm^2 and a maximum power density of 1.4 W cm^{-2} at 800 °C. There were, however, problems with reaction with the YSZ electrolyte to give $La_2Zr_2O_7$ at the interface at temperatures above 1000 °C.

In addition to the gallate materials, perovskite based rare earth aluminates have also attracted attention. Studies of a sample of $La_{0.9}Sr_{0.1}Al_{0.9}Mg_{0.1}O_{2.9}$ by Park *et al*, showed that below 550 °C, the total conductivity was dominated by the grain bound-

ary component, with this component decreasing substantially at high temperatures.[108] In this low temperature region, the grain boundary contribution was shown to be mainly ionic at low $p(O_2)$ and mixed conducting at high $p(O_2)$. Tsuji *et al.* have examined the conductivities of $SmAlO_3$ doped on the Al site with Ni, Mg, Zn.[109] The conductivity increased in the order Ni, Mg, Zn. From the oxygen partial pressure dependence it was shown that $SmAl_{0.95}Zn_{0.5}O_{3-x}$ was a mixed (oxide ion and hole) conductor with the oxide ion transport number increasing with decreasing temperature.

In terms of other perovskite related systems, doped $Ba_2In_2O_5$ continues to attract attention. Kaninuma *et al.* have examined the effect of doping with Sr and La, and found that the ionic conductivity increased with both La and Sr content.[110] The conductivity of the sample $Ba_{0.6}Sr_{0.4}LaIn_2O_{5.5}$ exceeded that of YSZ having a value of 0.12 S cm^{-1} at 1073 K. Correlation of oxide ion conductivities with free volume was discussed by the authors, and was shown to have a key effect.

Apatite-type oxide ion conductors (Fig. 4.) have attracted more attention this year, showing considerable promise as alternatives to fluorite or perovskite oxide ion conducting systems. Single crystal studies of the apatite type system $Nd_{9.33-x}(SiO_4)_6O_{2-3x/2}$ by Nakayama *et al.* have shown that the conductivity parallel to the crystallographic *c* axis is about 1 order of magnitude higher than that perpendicular[111] confirming the importance of the oxide ion channels running through the structure. Doping studies by McFarlane *et al.* have shown that it is possible to partially substitute Co, Fe and Mn on the Si site in $La_{9.33}Si_6O_{26}$.[112] All the doped phases showed high conductivities, with Co and Mn substitution introducing an additional electronic contribution to the conductivity. From chemical compatibility studies with present SOFC perovskite cathode materials, it was shown that these doped phases could form at the interface between apatite electrolytes and perovskite cathodes. The high

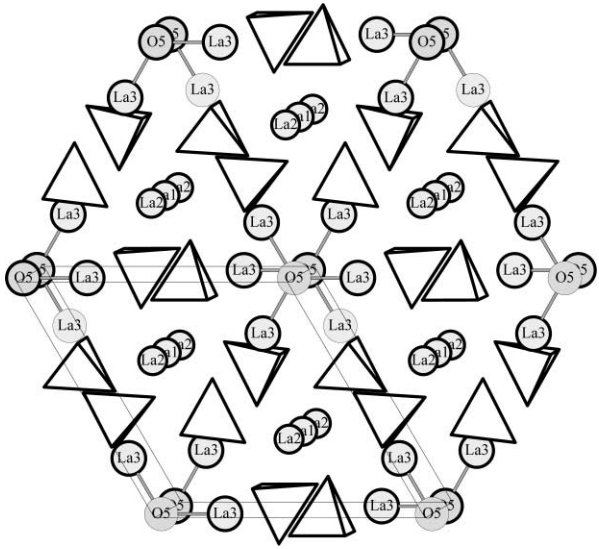

Fig. 4 The structure of the apatite-type oxide ion conductor, $La_{9.33}Si_6O_{26}$ (tetrahedra = SiO_4).

conductivities of the doped phases should, however, mean that this potential interfacial reaction is not likely to represent a significant problem in the use of apatite-type electrolytes in SOFCs.

Research has been performed on the replacement of Si by Ge in $La_{9.33}Si_6O_{26}$, although this Ge based system has attracted some confusion about the exact nature of the conducting phase. Ishihara *et al.* have reported that this phase is of the cation deficient $La_{2-x}GeO_{5-3x/2}$ type.[113] Doping with alkaline earths showed an increase in the conductivity at low temperatures, with the conductivity of the composition $La_{1.5}Ca_{0.2}GeO_{4.45}$ being higher than that of YSZ at all temperatures examined. In contrast to this particular report, reports by Sansom *et al.* and Berestagui *et al.* have claimed that the conducting phase is apatite-type.[114,115] Both groups have shown that single phase hexagonal apatite $La_{9.33}Ge_6O_{26}$ can be prepared at temperatures around 1150 °C. Heating to higher temperatures results in severe peak broadening/extra peaks in the X-ray powder diffraction pattern, although the pattern still resembles that of an apatite-type phase (possibly triclinic). In addition, a detailed investigation of La_2GeO_5 by Berastegui *et al.* claimed that the introduction of the cation vacancies reported by Ishihara *et al.* was not possible. The changes in the X-ray pattern of $La_{9.33}Ge_6O_{26}$ on heating to high temperatures have been attributed to Ge volatility and changes in the ordering along the apatite channels.

Other oxide ion conductors being investigated include $La_2Mo_2O_9$ type materials. Khadasheva *et al.* have examined a range of samples, $La_2(Mo_{1-x}M_x)_2O_9$ (M = Nb, Ta; $0 \leq x \leq 0.2$).[116] The introduction of 5 wt% Nb was shown to increase the conductivity at 800 °C. Arulraj *et al.* have succeeded in preparing F doped $La_2Mo_2O_9$. Low levels of fluorine were introduced, *i.e.* $La_2Mo_2O_{9-0.5x}F_x$ ($0.02 \leq x \leq 0.3$), and the doped samples showed a decrease in the transition temperature for the order–disorder structural transition.[117]

Takashima *et al.* have investigated the oxide ion conductivity of the oxide fluoride phase $La_2Eu_2O_3F_6$.[118] The crystal structure was shown to be a monoclinic variant of the fluorite structure. There appears to be greater disorder within this phase compared to $Nd_2Eu_2O_3F_6$, which displays higher oxide ion conductivity (2 S m^{-1} *versus* 0.8 S m^{-1} at 773 K), and it is suggested that this disorder may be responsible for the lower conductivity.

Interesting results have been reported for composite electrolytes containing an oxide ion conducting ceramic (*e.g.* doped CeO_2) and chloride or carbonate salts.[119,120] The composites showed higher ionic conductivities compared to doped ceria on its own. Such electrolytes have been examined in an intermediate temperature SOFC. The conductivity of the electrolyte (CeO_2–LiCl–$SrCl_2$) was 0.09–0.13 S cm^{-1} at 500–650 °C, and the cell generated a peak power density of 510 mW cm^{-2} with a current density of 1250 mA cm^{-2} at 625 °C, making it a potential material for low cost IT-SOFC systems.

Along with the considerable research on electrolyte materials for SOFCs, there is a corresponding strong focus on the development of new improved electrode materials. New anode materials are being sought for SOFCs due to problems with the existing anode Ni/YSZ cermet. This suffers from a number of deficiencies, including coking when used with hydrocarbon fuels. Replacement of Ni by Cu or Co is being investigated by a number of groups, reporting increased catalytic activity, along with reduced coking.[121,122,123,124,125,126] The results have shown that Cu/CeO_2/YSZ

composites show particularly promising potential for direct hydrocarbon oxidation in an SOFC.

In terms of the cathode material, composite $Sm_{0.5}Sr_{0.5}CoO_3/Sm_{0.2}Ce_{0.8}O_{1.9}$ cathodes have been investigated for use in low temperature (400–600 °C) SOFCs.[127] It was shown that the optimum $Sm_{0.2}Ce_{0.8}O_{1.9}$ content in the composite was about 30 wt %, leading to a dramatic improvement in the catalytic properties of the interfaces. Thangadurai *et al.* have examined the mixed conducting perovskites $SrSn_{1-x}Fe_xO_{3-y}$ ($0 \leq x \leq 1$).[128] The compounds with low Fe content were shown to exhibit both ionic and electronic conductivity, while the samples with higher Fe content were mainly electronic conductors. The perovskite $Sr_{0.8}Ce_{0.1}Fe_{0.7}Co_{0.3}O_{3-x}$, prepared by a modified citrate route, has also been examined as a cathode material in an intermediate temperature SOFC.[129] The material exhibited an area-specific resistivity of 0.86 Ω cm^2 at 700 °C.

In other research, a silver coating has been employed to improve the oxygen exchange reaction activity for a $La_{0.6}Sr_{0.4}Co_{0.8}Fe_{0.2}O_3$–$Ce_{0.8}Gd_{0.2}O_{1.9}$ composite cathode.[130] An interface conductivity greater than 1 S cm^{-1} was obtained at 600 °C with a low activation energy.

Murray *et al*. have presented results for $La_{0.6}Sr_{0.4}Co_{0.2}Fe_{0.8}O_3$ cathodes on YSZ, and shown lower low-current interfacial resistance values compared to LSM.[131] Use of a composite with $Ce_{0.8}Gd_{0.2}O_{1.9}$ resulted in an additional improvement. Hart *et al*. have shown improved properties by using functionally graded LSM and $Ce_{0.8}Gd_{0.2}O_{1.9}$ or YSZ mixtures.[132] The best cathodes were shown to be the ones containing $Ce_{0.8}Gd_{0.2}O_{1.9}$ particularly as the temperature was lowered towards 700 °C.

The mixed conducting material $Sr_4Fe_{6-x}Co_xO_{13+y}$ has continued to attract attention for potential use as an SOFC cathode material or an oxygen separation membrane. Manthiram *et al*. have shown that the high oxygen permeation flux of the high Co content phases ($x > 1.8$) is due to the presence of a perovskite secondary phase.[133] The authors have also investigated the Ruddlesden Popper type phases $(La,Sr)_{n+1}(Fe, Co)_nO_{3n+1-x}$. The $n = 1$ member is shown to exhibit negligible oxygen flux, while the $n = 2$, 3 phases exhibit oxygen fluxes one order of magnitude lower than the perovskite $SrCo_{0.8}Fe_{0.2}O_{3-x}$. The presence of La was shown to aid the structural stability at high temperature and low $p(O_2)$, with the composition $La_{0.3}Sr_{2.7}Fe_{1.4}Co_{0.6}O_{7-x}$ showing amongst the best properties. Deng *et al.* have also examined the multiphase $Sr_4Fe_{6-x}Co_xO_{13+y}$ system, and shown that the conductivity increases with Co content.[134] Unusual changes in the conductivities were observed at temperature around 900 °C, and it was suggested that this may be associated with conversion of the perovskite secondary phase into the layered $Sr_4Fe_{6-x}Co_xO_{13+y}$ type phase.

In related work, Wiik *et al.* have investigated oxygen permeation through $SrFeO_{3-x}$/$SrCoO_{3-y}$ solid solutions.[135] The oxygen flux rate was shown to increase with Co content, with a maximum for the composition with 67% Co. The results also showed a large reduction in oxygen flux below 900 °C for membranes with composition $Sr_{0.97}Fe_{0.33}Co_{0.67}O_{3-x}$ due to a transition from a cubic perovskite phase (disordered oxygen vacancies) to a rhombohedral brownmillerite phase (ordered oxygen vacancies). The phase $Sr_{0.25}Bi_{0.5}FeO_{3-x}$ has also been investigated as a cathode material for intermediate temperature SOFCs, as well as a membrane reactor material.[136] Results suggest that the interfacial resistances at low oxygen partial pressures limit the oxygen permeation rates.

In the same area, Jennings and Skinner have examined the conductivities of the K_2NiF_4 type phases $La_xSr_{2-x}FeO_{4+y}$.[137] The materials were shown to be stable under conditions applicable for SOFC cathode operation. The results suggested that oxygen excess was incorporated into interstitial sites within the lattice, and that the d.c. conductivity was significantly influenced by the oxygen content. Related to this material, Kilner and Shaw have examined the oxygen diffusion and surface exchange coefficients for $La_2Ni_{1-x}Co_xO_{4+y}$, which has the ability to incorporate excess oxygen in interstitial sites within the lattice.[138] Single phase samples were observed for $0 \leq x < 0.5$ and it was shown that the oxygen diffusion coefficient was fairly insensitive to the Co content. In contrast, Co doping was shown to significantly enhance the surface exchange coefficient, with a drop in the activation enthalpy for this process from 80 kJ mol^{-1} to values as low as 20 kJ mol^{-1} for the high Co content samples. Another interstitial oxide ion containing phase that has attracted attention is $CeTaO_{4+x}$ ($0.06 \leq x \leq 0.17$).[139] The conductivities obtained were relatively high, although further work is required to determine the exact nature of the conductivity.

In addition to cathode and anode materials, there is considerable interest in the optimisation of the SOFC interconnect material. At present the favoured material is a doped rare earth chromate perovskite. These chromates require very high sintering temperatures to obtain a dense material, and so there is currently a lot of interest in lowering the sintering temperature.[140,141,142,143] Kunifusa *et al.* have succeeded in preparing single phase perovskite systems $NdCr_{1-x}Mg_xO_3$ ($0 \leq x \leq 0.25$) at low temperatures from the decomposition of $NdCr_{1-x}Mg_xO_4$ prepared by the hydrazine method.[140] Dense pellets of these phases could be prepared by sintering at 1800 °C for 4 hours. The conductivity increased with increasing Mg content, with a value of 1.4×10^3 S m^{-1} at 1000 °C for $x = 0.25$. Mori *et al.* have investigated the air sintering of Al and Co doped $La_{1-x}Sr_xCrO_3$.[141] The sample $La_{0.9}Sr_{0.1}Cr_{0.95}Al_{0.2}Co_{0.2}O_3$ showed enhanced sintering with relative densities greater than 94% when sintered at 1600 °C for 20 hours. The surface was shown to be B site deficient due to Co evaporation. Similarly, small levels of V, Co, Ni doping were shown to enhance the air sintering characteristics of $La_{0.8}Sr_{0.2}Cr_{0.9}Ti_{0.1}O_3$, with V doping giving the greatest effect.[142] Ovenstone *et al.* have shown that a combination of hydrothermal processing followed by high temperature sintering resulted in dense pellets of $La_{0.7}Ca_{0.3}CrO_3$ and $La_{0.84}Sr_{0.16}CrO_3$ at lower temperatures than by conventional synthesis routes.[143]

Further work on supported mixed gas SOFCs was presented by Raz *et al.*[144] In these systems the anode and cathode are both exposed to the same mixture of gases, and the potential is generated due to the differences in catalytic activities between anode and cathode. Although some promising results were produced, the power density was small due to the high internal resistance of the cell.

To conclude this section on oxide ion conductors/solid oxide fuel cells, there has been a range of useful general articles published in the field of SOFCs. Haines *et al.* have reported the latest progress in the setting up of a demonstration natural gas fired 0.25 MW SOFC modified to enable capture of CO_2.[145] The system is a collaboration between Siemens Westinghouse and Shell International and is due to start up in Norway, and the authors discuss the scientific progress as well as the potential for stationary power generation using SOFC with CO_2 capture technology. Singhal has reviewed SOFCs for stationary, mobile and military applications.[146] The author suggests that the low power densities associated with tubular designs, mean that these are

only suitable for stationary power applications, while planar designs have some potential in mobile applications, such as auxiliary power units.

Colella has reviewed the potential for combined heat and power fuel cell systems, based on the current market position, with particular attention to the situation in the UK.[147] In further reviews, Winkler and Lorenz have discussed the design of stationary and mobile SOFC-gas turbine systems.[148]

10 H^+ ion conductors

As for oxide ion conductors, research on proton conducting solid electrolytes has been driven by their potential use in technological applications, such as SOFCs, hydrogen separation membranes. Perovskite-based materials remain the most widely researched in this area.

Hui and Michele have investigated the electrical properties of Bi-doped $BaCeO_3$.[149] Solid solutions of the form $BaCe_{1-x}Bi_xO_3$ ($0 \leq x \leq 0.5$) were successfully prepared, and it was shown that the presence of Bi helped to improve the chemical stability in the presence of moisture. Bi doping was also shown to increase the electronic conductivity, although the proton conductivity dropped significantly.

Irvine *et al.* have performed detailed structural studies of the perovskite-type proton conductors $Sr_3Ca_{1+x}Nb_{2-x}O_{9-y}$ and shown that the structures of the hydrated phases differ significantly from those of the samples without water.[150] Amongst the changes are subtle variations in unit cell symmetry due to octahedral tilting/distortion, oxygen vacancy filling/creation and cation displacements. The same group has reported a range of research on the complex proton conducting perovskite oxides $Sr_3CaZr_{1-x}Ta_{1+x}O_{8.5-x/2}$.[151,152] In addition to the preparation of dense films by a sol–gel route[151] the authors have shown that molecular species such as oxygen and carbonate may be incorporated into this system by heat treatment at high temperatures (>1000 °C) and/or pressures.[152] EPR studies on oxygenated samples suggest the presence of peroxidic groups.

Proton conduction in the perovskite-type compounds $La_{0.9}Sr_{0.1}MO_{3-x}$ (M = Sc, In, Lu) has been investigated by Nomura *et al.*[153]All samples were shown to exhibit significant proton conduction in wet atmospheres or H_2. The highest conductivity was observed for M = Sc, with a value of 4×10^{-3} S cm^{-1} at 873 K in the presence of water vapour or hydrogen. Increasing the size of the M cation resulted in a decrease in the proton conductivity.

Apparent hydride ion conduction has been reported by Wideroe *et al.* in Al-doped $SrTiO_3$.[154] Detailed transport number measurements, using the concentration cell/emf method in wet atmospheres as a function of $p(O_2)$, supported earlier indications of apparent negative transport by hydrogen at high temperatures under reducing conditions.

Shimura *et al.* have examined proton conduction in perovskite-related aluminates, $La_{n-x}Sr_{1+x}Al_nO_{3n+1-y}$ ($n = 1, 2$).[155] For these phases, the highest conductivity was observed for $La_{0.9}Sr_{1.1}AlO_{3.95}$ with a value of 2.4×10^{-4} S cm^{-1} at 1273 K in H_2, with a range of measurements supporting the conclusion of a contribution from proton conduction. The same group has examined the proton conduction of the perovskite systems $AZrO_3$ (A = Ba, Sr, Ca) doped with Rh.[156] Proton conductivities in hydrogen

were close to that of Y doped $AZrO_3$. Conductivities in high oxygen partial pressures were lower than for Y doped $AZrO_3$, which was attributed to a change in the valence of Rh suppressing the generation of holes, and so giving rise to reduced hole conduction.

Kroger *et al.* have investigated the ion transport in the hydrogen fluorides KHF_2, NH_4HF_2, $BaHF_3$ as a function of temperature in the presence of HF and H_2O.[157] A range of measurements were performed with different electrode materials to determine the degree of proton and fluoride ion conductivity. Results indicated that all materials showed significant proton conduction, with fluoride ion conduction also observed in the case of $BaHF_3$. $BaHF_3$ only exhibited significant conductivity when exposed to HF- or H_2O-containing atmospheres, whereas NH_4FHF_2 showed some conductivity in dry atmospheres, indicating intrinsic proton mobility.

$LiF–MgF_2$ composites have been shown to exhibit high ionic conductivity (10^{-2}–10^{-1} S cm^{-1} at 600–800 °C).[158] The high ionic conductivity of the composite compared to the individual phases was attributed to a mechanism involving conduction mainly through the interfacial region between LiF and MgF_2 grains. From experimental results the authors suggest that proton conduction dominates in this system.

In terms of applications, Hibino *et al*. have examined the characteristics of a low temperature (350–600 °C) SOFC with $BaCe_{1-x}Y_xO_{3-y}$ as an electrolyte, a Pd loaded FeO anode, and $Ba_{0.5}Pr_{0.5}CoO_3$ as the cathode.[159] The resulting power density was higher than observed at comparable temperatures for SOFCs using zirconia or ceria based electrolytes. In other areas, research by Sakaguchi *et al*. has suggested that the perovskite material $SrCe_{0.95}Yb_{0.05}O_3$ can absorb and desorb hydrogen electrochemically like hydrogen storage alloys.[160] As a result the authors examined anode composite materials containing the perovskite and hydrogen storage alloys and found an enhanced activation performance in a Ni-metal hydride battery.

11 Other cation conductors

Ball milling has been used to prepare Ag ion conducting $Ag_2S–SiS_2$ systems with the composition of Ag_2S being varied from 0 to 60 mol%.[161] The conductivity was shown to increase with Ag_2S content, with the 60 mol% sample showing a conductivity of 6.9×10^{-2} S cm^{-1} at 298 K.

Further results on possible trivalent cation conduction in NASICON systems, $Sc_{0.33}Zr_2(PO_4)_3$ have been reported.[162,163] Evidence for trivalent cation conduction was provided by d.c. electrolysis results. The NASICON type systems were reported to be more promising for device applications than $Sc_2(WO_4)_3$, due to a higher relative density and hardness.

12 Superconductivity

One of the most significant factors to occur in the literature in 2002 was the discreditation of a number of important papers from previous years. A full discussion of this topic is beyond the scope of this report. More information can be found in reference 164.

In terms of published results, superconductivity has been demonstrated in Li under high pressures. Struzhkin *et al.* reported T_c's ranging from 9 to 16 K at 23 to 80 GPa.[165] These T_c's are lower than predicted from theory, and so suggest that more sophisticated theoretical interpretations are required. Shimuzu *et al*. have also reported superconductivity in Li under high pressure, with a T_c of 20 K at 48 Gpa, which represents the highest T_c of any element.[166]

Sarrao *et al*. have observed superconductivity at 18 K in the plutonium-containing system $PuCoGa_5$.[167] The authors suggest that the observed superconducting properties derive directly from plutonium's anomalous electronic properties, and that the mechanism is unconventional with the transition temperature being substantially higher than that seen in U- and Ce-based heavy fermion systems.

Lobring *et al.* have prepared large single crystals of the superconducting phase V_2Ga_5.[168] The material is a type II superconductor with a transition temperature of 3.59 K. Computational studies have shown that the majority states at the Fermi level are associated with the V d-band.

In terms of synthesis routes to superconductors, Mandal *et al*. have prepared $La_{2-x}A_xCuO_4$ (A = Sr, Ba) samples using a novel metathesis route involving the reaction of Li_2CuO_2 with alkaline earth doped LaOCl.[169] Using this route a new lithium substituted sample, $La_{1.8}Li_{0.2}CuO_4$ was also prepared.

References

1 M. Morcrette, Y. Chabre, G. Vaughan, G. Amatucci, J.-B. Leriche, S. Patoux, C. Masquelier and J. M. Tarascon, *Electrochimica Acta.*, 2002, **47**, 3137.
2 K. Kinoshita and K Zaghib, *J. Power Sources*, 2002, **110**, 416.
3 D. Aurbach, E. Zinigrad, Y. Cohen and H. Teller, *Solid State Ionics*, 2002, **148**, 405.
4 H. Li, Hong, L. Shi, Q. Wang, L. Chen and X Huang, *Solid State Ionics*, 2002, **148**, 247.
5 Z. Yang, H. Q. Wu and B Simard, *Electrochem. Commun.*, 2002, **4**, 574.
6 T. Abe, K. Takeda, T. Fukutsuka, Y. Iriyama, M. Inaba and Z. Ogumi, *Electrochem. Commun.*, 2002, **4**, 310.
7 P. Azais, L. Duclaux, A.-M. Faugere and F. Beguin, *Appl. Phys. Lett.*, 2002, **81**, 775.
8 O. Pan, K. Guo, L. Wang, Lingzhi and S. Fang, *Solid State Ionics*, 2002, **149**, 193.
9 S. Komaba, T. Ohtsuka, B. Kaplan, T. Itabashi, N. Kumagai and H. Groult, *Chem. Lett.*, 2002, 1236.
10 S. S. Zhang and T. R. Jow, *J. Power Sources*, 2002, **109**, 422.
11 H. Tostmann, A. J. Kropf, C. S. Johnson, J. T. Vaughey and M. M. Thackeray, *Phys. Rev. B.*, 2002, **66**, 14106/1.
12 M. Wachtler, M. Winter and J. Besenhard, *J. Power Sources*, 2002, **105**, 151.
13 N. Tamura, R. Ohshita, M. Fujimoto, S. Fujitani, M. Kamino and I. Yonezu, *J Power Sources*, 2002, **107**, 48.
14 G. A. Roberts, E. J. Cairns and J. A. Reimer, *J. Power Sources*, 2002, **110**, 424.
15 L. Monconduit, J. C. Jumas, R. Alcantara, J. L. Tirado and C. Perez Vicente, *J. Power Sources*, 2002, **107**, 74.
16 M.-L. Doublet, F. Lemoigno, F. Gillot and L. Monconduit, *Chem. Mater.*, 2002, **14**, 4126.
17 V. Pralong, D. C. S. Souza, K. T. Leung and L. F. Nazar, *Electrochem. Commun.*, 2002, **4**, 516.
18 J. Yang, Y. Takeda, N Imanishi, C. Capiglia, J. Xie and O. Yamamoto, *Solid State Ionics*, 2002, **152–153**, 125.
19 D. Aurbach, A. Nimberger, B. Markovsky, E. Levi, E. Sominski and A. Gedanken, *Chem. Mater.*, 2002, **14**(10), 4155.
20 M. Martos, J. Morales and J. L. Sanchez, *J. Mater. Chem.*, 2002, **12**, 2979.
21 D. Hara, H. Ikuta, Y. Uchimoto and M. Wakihara, *J. Mater. Chem.*, 2002, **12**, 2507.
22 S.-S. Kim, S. Ogura, H. Ikuta, Y. Uchimoto and M. Wakihara, *Solid State Ionics*, 2002, **146**, 249.
23 M. Behm and J. T. S. Irvine, *Electrochimica Acta*, 2002, **47**, 1727.
24 A. Palos, M. Ibarra, M. Morcrette and P. Strobel, *J. Solid State Electrochem.*, 2002, **6**, 134.
25 G. X. Wang, Y. Chen, K. Konstantinov, M. Lindsay, H. K. Liu and S. X. Dou, *J. Power Sources*, 2002, **109**, 142.

26 G. X. Wang, Y. Chen, K. Konstantinov, J. Yao, J.-h. Ahn, H. K. Liu and S. X. Dou, *J. Alloys Compd.*, 2002, **340(1–2)**, L5.
27 H. Li, Q. Wang, L. Shi, L. Chen and X. Huang, *Chem. Mater.*, 2002, **14**, 103.
28 W. X. Chen, J. Y. Lee and Z. Liu, *Electrochem Commun.*, 2002, **4**, 260.
29 M. Egashira, H. Takatsuji, S. Okada and J. Yamaki, *J. Power Sources*, 2002, **107**, 56.
30 A. Dailly, P. Willmann and D. Billaud, *Electrochimica Acta*, 2002, **48**, 271.
31 H. Fujimoto, A. Mabuchi, C. Natarajan and T. Kasuh, *Carbon*, 2002, **40**, 567.
32 Y. M. Hon, K. Z. Fung, S. P. Lin and M. H. Hon, *J. Solid State Chem.*, 2002, **163**, 231.
33 W. Tang, X. Yang, Z. Liu, S. Kasaishi and K. Ooi, *J. Mater. Chem.*, 2002, **12**, 2991.
34 M. A. Monge, J. M. Amarilla, E. Gutierrez-Puebla, J. A. Campa and I. Rasines, *ChemPhysChem*, 2002, **3**, 367.
35 D. Singh, W.-S. Kim, V. Craciun, H. Hofmann and R. K. Singh, *Appl. Surf. Sci.*, 2002, **197–198**, 516.
36 C. Julien, I. Ruth Mangani, S. Selladurai and M. Massot, *Solid State Sci.*, 2002, **4**, 1031.
37 L. Hernan, J. Morales, L. Sanchez, E. R. Castellon and M. A. G. Aranda, *J Mater. Chem.*, 2002, **12**, 734.
38 H. Shigemura, M. Tabuchi, K. Mitsuharu; H. Sakaebe, A. Hirano and H. Kageyama, *J. Mater. Chem.*, 2002, **12**, 1882.
39 Z. Liu, H. Wang, L. Fang, J. Y. Lee and L. M. Gan, *J. Power Sources*, 2002, **104**, 101.
40 H. Tang, C. O. Feng, O. L. Fan, T. M. Lei, J. T. Sun, L. J. Yuan and K. L. Zhang, *Chem. Lett.*, 2002, **8**, 822.
41 C.-H. Han, Y.-S. Hong, H.-S. Hong and K. Kim, *J. Power Sources*, 2002, **111**((1)), 176.
42 A. R. Armstrong, A. J. Paterson, A. D. Robertson and P. G. Bruce, *Chem. Mater.*, 2002, **14**((2)), 710.
43 Z. P. Guo, S. Zhong, G. X. Wang, G. Walter, H. K. Liu and S. X. Dou, *J. Electrochem. Soc.*, 2002, **149**, A792.
44 S.-J. Hwang, H.-S. Park and J.-H. Choy, *Solid State Ionics*, 2002, **151**, 275.
45 S.-T. Myung, S. Komaba and N. Kumagai, *Electrochimica Acta*, 2002, **47**, 3287.
46 S. Komaba, S.-T. Myung, N. Kumagai, T. Kanouchi, K. Oikawa and T. Kamiyama, *Solid State Ionics*, 2002, **152–153**, 311.
47 S.-T. Myung, S. Komaba and N. Kumagai, *J. Electrochem. Soc.*, 2002, **149**, A1349.
48 S.-T Myung, S. Komaba and N. Kumagai, *Solid State Ionics*, 2002, **150**, 199.
49 Y.-S. Lee, *Chem. Lett.*, 2002, **12**, 1228.
50 J. Cho, Y. J. Kim, T.-J. Kim and B. Park, *J. Electrochem. Soc.*, 2002, **149**, A127.
51 J. Cho, T.-J. Kim and B. Park, *J. Electrochem. Soc.*, 2002, **149**, A288.
52 S.-K. Chang, H.-J. Kweon, B.-K. Kim, D.-Y. Jung and Y.-U. Kwon, *J. Power Sources*, 2002, **104**, 125.
53 A. Burukhin, O. Brylev, P. Hany and B. R. Churagulov, *Solid State Ionics*, 2002, **151**, 259.
54 W. T Jeong and K. S. Lee, *J. Power Sources*, 2002, **104**, 195.
55 K. Kushida and K. Kuriyama, *J. Crystal Growth*, 2002, **237–239**, 612.
56 J. Pracharova, J. Pridal, J. Bludska, I. Jakubec, V. Vorlicek, Z. Malkova, Th. M. Dikonimos, R. Giorgi and L. Jastrabik, *J. Power Sources*, 2002, **108**, 204.
57 K. J. Rao, H. Benqlilou-Moudden, G. Couturier, P. Vinatier and A. Levasseur, *Mater. Res. Bull.*, 2002, **37**, 1353.
58 P. J. Bouwman, B. A. Boukamp, H. J. M. Bouwmeester and P. H. L. Notten, *Solid State Ionics.*, 2002, **152–153**, 181.
59 Z. Wang, L. Liu, L. Chen and X. Huang, *Solid State Ionics*, 2002, **148**, 335.
60 L. Liu, Z. Wang, H. Li, L. Chen and X. Huang, *Solid State Ionics*, 2002, **152–153**, 341.
61 T. Fujiwara, Y. Nakagawa, T. Nakaue, S.-W. Song, T. Watanabe, R. Teranishi and M. Yoshimura, *Chem. Phys. Lett.*, 2002, **365**, 369.
62 M. Y. Song and R. Lee, *J. Power Sources*, 2002, **111**, 97.
63 C.-C. Chang, J. Y. Kim and P. N. Kumta, *J. Electrochem. Soc.*, 2002, **149**, A1114.
64 H.-K. Kim, T.-Y. Seong and Y.-S. Yoon, *Electrochem. Solid-State Lett.*, 2002, **5**, A252.
65 H. Arai, M. Tsuda, K. Saito, M. Hayashi and Y. Sakurai, *J. Electrochem. Soc.*, 2002, **149**, A401.
66 H. Arai, M. Tsuda, K. Saito, M. Hayashi and Y. Sakurai, *Electrochim. Acta*, 2002, **47**, 2697.
67 R. Moshtev, P. Zlatilova, I. Bakalova and S. Vassilev, *J. Power Sources*, 2002, **112**, 30.
68 L. Zhang, H. Noguchi and M. Yoshio, *J. Power Sources*, 2002, **110**, 57.
69 R. Chitrakar, S. Kasaishi, A. Umeno, K. Sakane, N. Takagi, Y.-S. Kim and K. Ooi, *J. Solid State Chem.*, 2002, **169**, 35.
70 S.-S. Shin, Y.-K. Sun and K. Amine, *J. Power Sources*, 2002, **112**, 634.
71 S.-H. Kang, J. Kim, M. E. Stoll, D. Abraham, Y. K. Sun and K. Amine, *J. Power Sources*, 2002, **112**, 41.
72 R. Ulrich, J. W. Zwanziger, S. M. De Paul, A. Reiche, H. Leuninger, H. W. Spiess, U. Wiesner and Ulrich, *Adv. Mater.*, 2002, **14**, 1134.
73 Q. Li, N. Imanishi, A. Hirano, Y. Takeda and O. Yamamoto, *J. Power Sources*, 2002, **110**, 38.
74 M.-K. Song, J.-Y. Cho, B. W. Cho and H. W. Rhee, *J. Power Sources*, 2002, **110**, 209.
75 W. Xu and C. A. Angell, *Solid State Ionics*, 2002, **147**, 295.
76 Y. Wang, J. Travas-Sejdic and R. Steiner, *Solid State Ionics*, 2002, **148**, 443.
77 H.-H. Kuo, W.-C. Chen, T.-C Wen and A. Gopalan, *J. Power Sources*, 2002, **110**, 27.
78 M. Murayama, R. Kanno, M. Irie, S. Ito, T. Hata, N. Sonoyama and Y. Kawamoto, *J. Solid State Chem.*, 2002, **168**, 140.

79 M. Murayama, R. Kanno, Y. Kawamoto and T. Kamiyama, *Solid State Ionics*, 2002, **154**, 789.
80 K. Arbi, M. Ayada-Trabelsi and J. Sanz, *J. Mater. Chem*, 2002, **12**, 2985.
81 K. Arbi, S. Mandal, J. M. Rojo and J. Sanz, *Chem. Mater.*, 2002, **14**, 1091.
82 Y. Inaguma, T. Katsumata, M. Itoh and Y. Morii, *J. Solid State Chem.*, 2002, **166**, 67.
83 M. Nakayama, H. Ikuta, Y. Uchimoto and M. Wakihara, *J. Mater. Chem.*, 2002, **12**, 1500.
84 A. Morata-Orrantia, S. Garcia-Martin, E. Moran and M. A. Alario-Franco, *Chem. Mater.*, 2002, **14**, 2871.
85 L. Sebastian, J. Gopalakrishnan and Y. Piffard, *J. Mater. Chem.*, 2002, **12**, 374.
86 I. Kosacki, H. U. Andreson, Y. Mizutani and K. Utai, *Solid State Ionics*, 2002, **152**, 431.
87 Z. Cai, T. N. Lan, S. Wang and M. Dokiya, *Solid State Ionics*, 2002, **152**, 583.
88 K. Kobayashi, I. Takahashi, M. Shiono and M. Dokiya, *Solid State Ionics*, 2002, **152**, 591.
89 S. Tao and J. T. S. Irvine, *J. Solid State Chem.*, 2002, **165**, 12.
90 S. Dikmen, P. Shuk, M. Greenblatt and H. Gocmez, *Solid State Sciences*, 2002, **4**, 585.
91 S. G. Kim, S. P. Yoon, S. W. Nam, S. H. Hyun and S. A. Hong, *J. Power Sources*, 2002, **110**, 222.
92 E. D. Wachsman, *Solid State Ionics*, 2002, **152**, 657.
93 N. X. Jiang, E. D. Wachsman and S. H. Jung, *Solid State Ionics*, 2002, **150**, 347.
94 S. Uma, R. Bliesner and A. W. Sleight, *Solid State Sci.*, 2002, **4**, 329.
95 J. Grins, S. Esmaeilzadeh and S. Hull, *J. Solid State Chem.*, 2002, **163**, 144.
96 A. Watanabe and K. Das, *J. Solid State Chem.*, 2002, **163**, 224.
97 I. Abrahams and F. Krok, *J. Mater. Chem.*, 2002, **12**, 3351.
98 K. Yamaji, T. Horita, N. Sakai and H. Yokokawa, *Solid State Ionics*, 2002, **152**, 517.
99 J. H. Jang and G. M. Choi, *Solid State Ionics*, 2002, **154**, 481.
100 M. Rozumek, P. Majewski, T. Maldener and F. Aldinger, *Materialwiss. Werkstofftech*, 2002, **33**, 348.
101 T. Fukui, S. Ohara, K. Murata, H. Yoshida, K. Miura and T. Inagaki, *J. Power Sources*, 2002, **106**, 142.
102 J. W. Yan, Z. G. Lu, Y. Jiang, Y. L. Dong, C. Y. Yu and W. Z. Li, *J. Electrochem. Soc.*, 2002, **149**, A1132.
103 T. Ishihara, S. Fukui, H. Nishiguchi and Y. Takita, *J. Electrochem Soc.*, 2002, **149**, A823.
104 T. Ishihara, S. Fukui, H. Nishiguchi and Y. Takita, *Solid State Ionics*, 2002, **152**, 609.
105 T. Ishihara, Y. Tsuruta, T. Todaka, H. Nishiguchi and Y. Takita, *Solid State Ionics*, 2002, **152**, 709.
106 T. Ishihara, Y. Tsuruta, C. Y. Yu, T. Todaka, H. Nishiguchi and Y. Takita, *J. Electrochem. Soc.*, 2002, **150**, E17.
107 T. J. Armstrong and A. V. Vickar, *J. Electrochem Soc.*, 2002, **149**, A1565.
108 J. Y. Park and G. M. Choi, *Solid State Ionics*, 2002, **154**, 535.
109 T. Tsuji, Y. Ohashi and Y. Yamamura, *Solid State Ionics*, 2002, **154**, 541.
110 K. Kaninuma, H. Yamamura, H. Haneda and T. Atake, *Solid State Ionics*, 2002, **154**, 571.
111 S. Nakayama, M. Higuchi and K. Uematsu, *Nippon Kagaku Kaihi*, 2002, **2**, 243.
112 J. McFarlane, S. Barth, M. Swaffer, J. E. H. Sansom and P. R. Slater, *Ionics*, 2002, **8**, 149.
113 T. Ishihara, H. Arikawa, T. Akbay, H. Nishiguchi and Y. Takita, *Solid State Ionics*, 2002, **154**, 455.
114 J. E. H. Sansom, L. Hildebrandt and P. R. Slater, *Ionics*, 2002, **8**, 155.
115 P. Berestegui, S. Hull, F. J. Garcia Garcia and J. Grins, *J. Solid State Chem.*, 2002, **168**, 294.
116 Z. S. Khadasheva, N. U. Venskovskii, M. G. Safronenko, A. V. Mosunov, E. D. Politova and S. Y. Stefanovich, *Inorg. Mater.*, 2002, **38**, 1168.
117 A. Arulraj, F. Goutenoire, M. Tabellout, O. Bohnke and P. Lacorre, *Chem. Mater.*, 2002, **14**, 2492.
118 M. Takashima, S. Yonezawa and M. Leblanc, *Solid State Ionics*, 2002, **154**, 547.
119 G. Y. Meng, Q. X. Fu, S. W. Zha, C. R. Xia, Q. X. Liu and D. K. Peng, *Solid State Ionics*, 2002, **148**, 533.
120 Q. X. Fu, S. W. Zha, W. Zhang, D. K. Peng, G. Y. Meng and B. Zhu, *J. Power Sources*, 2002, **104**, 73.
121 M. K. Dongare, A. M. Dongare, V. B. Tare and E. Kemnitz, *Solid State Ionics*, 2002, **152**, 455.
122 C. Lu, W. L. Worrell, C. Wang, S. Park, H. Kim, J. M. Vohs and R. J. Gorte, *Solid State Ionics*, 2002, **152**, 393.
123 R. J. Gorte, H. Kim and J. M. Vohs, *J. Power Sources*, 2002, **106**, 10.
124 B. Lindstrom and L. J. Petterson, *J. Power Sources*, 2002, **106**, 264.
125 H. Kim, C. Lu, W. L. Worrell, J. M. Vohs and R. J. Gorte, *J. Electrochem. Soc.*, 2002, **149**, A247.
126 O. Kazuhito and K. Sato, *J. Ceram. Process. Res.*, 2002, **3**, 114.
127 C. R. Xia, W. Rauch, F. L. Chen and M. L. Liu, *Solid State Ionics*, 2002, **149**, 11.
128 V. Thangadurai, P. Schmid-Beurmann and W. Weppner, *Mater. Res. Bull.*, 2002, **37**, 599.
129 M. T. Colomer, B. C. H. Steele and J. A. Kilner, *Solid State Ionics*, 2002, **147**, 41.
130 S. R. Wang, T. Kato, S. Nagata, T. Honda, T. Kaneko, N. Iwashita and M. Dokiya, *Solid State Ionics*, 2002, **146**, 203.
131 E. P. Murray, M. J. Sever and S. A. Barnett, *Solid State Ionics*, 2002, **148**, 27.
132 N. T. Hart, N. P. Brandon, M. J. Day and N. Lapena-Rey, *J. Power Sources*, 2002, **106**, 42.
133 A. Manthiram, F. Prado and T. Armstrong, *Solid State Ionics*, 2002, **152**, 647.
134 Z. Q. Deng, G. G. Zhang, W. Liu, D. K. Peng and C. S. Chen, *Solid State Ionics*, 2002, **152**, 735.
135 K. Wiik, S. Aasland, H. L. Hansen, I. L. Tangen and R. Odegard, *Solid State Ionics*, 2002, **152**, 675.
136 X. Y. Lu and M. L. Liu, *Solid State Ionics*, 2002, **149**, 299.
137 A. J. Jennings and S. J. Skinner, *Solid State Ionics*, 2002, **152**, 663.
138 J. A. Kilner and C. K. M. Shaw, *Solid State Ionics*, 2002, **154**, 523.

139 S. J. Skinner, *Solid State Ionics*, 2002, **154**, 325.
140 Y. Kunifusa, M. Yoshinaka, K. Hirota and O. Yamaguchi, *Solid State Ionics*, 2002, **149**, 107.
141 M. Mori and N. M. Sammes, *Solid State Ionics*, 2002, **146**, 301.
142 M. Mori, *J. Electrochem. Soc.*, 2002, **149**, A797.
143 J. Ovenstone, K. C. Chan and C. B. Ponton, *J. Mater. Sci.*, 2002, **37**, 3315.
144 S. Raz, M. J. G. Jak, J. Schoonman and I. Riess, *Solid State Ionics*, 2002, **149**, 335.
145 M. R. Haines, W. K. Heidug, K. J. Li and J. B. Moore, *J. Power Sources*, 2002, **106**, 377.
146 S. C. Singhal, *Solid State Ionics*, 2002, **152**, 405.
147 W. Colella, *J. Power Sources*, 2002, **106**, 397.
148 W. Winkler and H. Lorenz, *J. Power Sources*, 2002, **105**, 222.
149 Z. Hui and P. Michele, *J. Mater. Chem*, 2002, **12**, 3787.
150 J. T. S. Irvine, D. J. D. Corcoran and J. Canales-Vazque, *Solid State Ionics*, 2002, **152**, 749.
151 C. Savaniu and J. T. S. Irvine, *Solid State Ionics*, 2002, **150**, 295.
152 J. T. S. Irvine, D. J. D. Corcoran, A. Lashtabeg and J. C. Walton, *Solid State Ionics*, 2002, **154**, 447.
153 K. Nomura, T. Takeuchi, S. Tanase, H. Kageyama, K. Tanimoto and Y. Miyazaki, *Solid State Ionics*, 2002, **154**, 647.
154 M. Wideroe, W. Munch, Y. Larring and T. Norby, *Solid State Ionics*, 2002, **154**, 669.
155 T. Shimura, Y. Tokiwa and H. Iwahara, *Solid State Ionics*, 2002, **154**, 653.
156 T. Shimura, K. Esaka, H. Matsumoto and H. Iwahara, *Solid State Ionics*, 2002, **149**, 237.
157 C. Kroger, H. Niggemeier, H. D. Wiemhofer, O. Glumov and I. Murin, *Solid State Ionics*, 2002, **154**, 487.
158 B. Zhu, Q. X. Fu, G. Y. Meng, J. F. Jurado, I. Albinsson and B. E. Mellander, *Solid State Ionics*, 2002, **148**, 583.
159 T. Hibino, A. Hashimoto, M. Suzuki and M. Sano, *J. Electrochem. Soc.*, 2002, **149**, A1503.
160 H. Sakaguchi, K. Hatakeyama, S. S. Kobayashi and T. Esaka, *Mater. Res. Bull.*, 2002, **37**, 1547.
161 H. F. Peng, N. Machida and T. Shiematsu, *J. Mater. Chem.*, 2002, **12**, 1094.
162 S. Tamura, N. Imanaka and G. Adachi, *Solid State Ionics*, 2002, **154**, 767.
163 N. Imanaka and G. Y. Adachi, *J. Alloys Compd.*, 2002, **344**, 137.
164 http://www.lucent.com/news_events/researchreview.html.
165 V. V. Struzhkin, M. I. Eremets, W. Gan, H. K. Mao and R. J. Hemley, *Science*, 2002, **298**, 1213.
166 K. Shimizu, H. Ishikawa, D. Takao, T. Yagi and K. Amaya, *Nature*, 2002, **419**, 597.
167 J. L. Sarrao, L. A. Morales, J. D. Thompson, B. L. Scott, G. R. Stewart, F. Wastin, J. Rebizant, P. Boulet, E. Colineau and G. H. Lander, *Nature*, 2002, **420**, 297.
168 K. C. Lobring, C. E. Check, J. H. Zhang, S. J. Li, C. Zheng and K. Rogacki, *J. Alloys Compd.*, 2002, **347**, 72.
169 T. K. Mandal, N. Y. Vasanthacharya and J. Gopalakrishnan, *J. Mater. Chem.*, 2002, **12**, 635.